https://doi.org/10.17221/147/2024-SWR

Contribution to the understanding of sediment transport during extreme flood event in Wei Laing watershed, East Nusa Tenggara, Indonesia

Muhammad Anggri Setiawan[1,2], Ratih Winastuti[2], Dimas Maula Hayat[2], Boma Karunia Dwi Putra[1,2], Djati Mardiatno[1]*, Nugroho Christanto[1,2], Meilinarti[3], Ida Ngurah[3]*

[1]*Department of Environmental Geography, Faculty of Geography, Gadjah Mada University, Yogyakarta, Indonesia*
[2]*Center for Disaster Studies, Gadjah Mada University, Yogyakarta, Indonesia*
[3]*Yayasan PLAN International Indonesia, Pasar Minggu, Jakarta Selatan, Indonesia*

**Corresponding authors: anggri@ugm.ac.id; djati.mardiatno@ugm.ac.id*

Citation: Setiawan M.A., Winastuti R., Hayat D.M., Putra B.K.D., Mardiatno D., Christanto N., Meilinarti, Ngurah I. (2025): Contribution to the understanding of sediment transport during extreme flood event in Wei Laing watershed, East Nusa Tenggara, Indonesia. Soil & Water Res., 20: 119–130.

Abstract: The 2021 Cyclone Seroja was a category 3 storm that made landfall on Lembata Island, causing extensive damage. This study aims to identify key interpretations of sediment transport related to tropical cyclones (TC) Seroja and past floods using a geopedological approach, estimate the return period through frequency analysis, and determine the rainfall threshold for flooding using HEC-RAS software. Extreme rainfall data from global precipitation model (GPM) (2000–2023) in Wei Laing watershed were analysed alongside LiDAR terrain data, physical and chemical properties of soil, and land cover data. Based on geopedological analysis, the result shows that the erosional-transfer zone of Wei Laing Watershed has thin, loamy, and slightly sandy soils due to erosion and limited pedogenesis. The depositional zone contains flood deposits with abrupt vertical texture changes, reflecting transported coarse grains and finer in-situ sediments. The modern flood deposit (TC Seroja flood deposit) was identified by texture, $CaCO_3$ content, organic matter, and coarse organic material. The fine-grained flood deposits (≤ 4 cm) are classified as slackwater deposits, consist of silty clay loam and silt loam textures, reflecting deposition under slow-flowing conditions. TC Seroja corresponds to a 50-year return period. Hydrological modelling indicates a 60 mm/day rainfall threshold for flooding, with 77 flood events recorded between 2000–2023. The model is confirmed by thick past flood deposits enriched with coarse organic materials. These findings provide insight into flood dynamics and sedimentary responses, supporting future flood risk mitigation efforts.

Keywords: flood deposition; Fluvial geomorphology; HEC-RAS; paleofloods; return period; tropical cyclones

The frequency and intensity of maritime disasters have increased due to climate change. Tropical cyclones (TC) have become one of the deadliest extreme events (Chen et al. 2024) and a serious threat to coastal communities (Shashank et al. 2024). The impacts of tropical cyclones also result in sediment transport, changes in salinity in tidal areas (Janakiraman et al. 2024), as well as shifts in coastlines and

Supported by the 2024 Academic Excellence Research Enhancement Grant Program, No. 6513/UN1.P1/PT.01.01/2024 from Universitas Gadjah Mada.

https://doi.org/10.17221/147/2024-SWR

coastal community structures (Eberenz et al. 2021). Although climate change has been a global threat since the mid-20th century, developing countries are projected to be the hardest hit due to their limited adaptive capacity (Dong et al. 2024). Indonesia is among the countries most vulnerable to climate change and natural disasters (Stanton-Geddes & Vun 2019; Fahrudin et al. 2022). Approximately 51 TCs were recorded entering Indonesia's southern regions from 1983 to 2017 (Mulyana et al. 2018). In the area around East Nusa Tenggara (NTT), several tropical cyclones have occurred, including TC Flores (1973), TC Bonnie (2002); TC Inigo (2003); TC Kirrily (2009); TC Frances (2017), and TC Seroja (2021) (Bureau of Meteorology 2023). The periodic occurrence of cyclones is a characteristic of the coastal areas in East Nusa Tenggara (NTT), given its position along the tropical storm tracks of the Timor Sea and the Indian Ocean. Tropical cyclone activity in NTT is influenced by its location near the equator (Sekaranom et al. 2021) and complex climate conditions, including sea surface anomalies, the Madden-Julian Oscillation, and equatorial convection (Kurniawan et al. 2021; Latos et al. 2023). Studies to understand the characteristics and mechanisms of the impacts of tropical cyclone phenomena in NTT are crucial as their intensity and frequency continue to rise.

Tropical cyclones cause more damage through storm surges and flooding than through strong winds. Therefore, areas vulnerable to TC landfalls may hold long-term geological records in the form of sediments, as these deposits result from storm-induced processes. Prehistoric tropical cyclone records can also be preserved as coastal geomorphological features (Nott 2004). Paleotempestology, the study of past storm activity, uses geological and geomorphological proxies from before observational records were available (Minamidate & Goto 2024). Over the decades, research on reconstructing flood records or paleohurricane archives has advanced significantly, including through sediment deposits (Rodysill et al. 2020), tree rings (Ballesteros-Canovas et al. 2020), and speleothem (Denniston & Luetscher 2017). However, long-term geological studies of tropical cyclones often face limitations in deciphering flood intensity (Donnelly et al. 2015). Records indicate significant changes in tropical cyclone activity alongside relatively sparse observational records, highlighting the need to detect long-term trends and correlate them with recurrence intervals. Geopedological approaches (geomorphology and pedology) are still rarely used to reconstruct flood disasters in tropical dry regions. We analysed paleoflood hydrology by integrating paleotempestology findings into flood inundation modelling to identify geomorphological records that can serve as paleoflood proxies. Therefore, the objectives of this study are: (1) to identify key interpretations of sediment transport related to TC Seroja and past floods using a geopedological approach; (2) to c estimates the return period through frequency analysis; and (3) to determines the rainfall threshold for flooding using HEC-RAS software.

MATERIAL AND METHODS

Study area. This research was conducted in Wowong Village, which was affected by flash floods caused by Cyclone Seroja in 2021 (Figure1). Wowong Village is part of the Wei Laing watershed, characterized by a complex topography with fluvial-marine plains surrounded by hills, and a bottleneck at the entrance to the village. The Wei Laing watershed covers an area of 11 000 km^2, with a climate influenced by monsoon and trade winds for 4–5 months. According to the geological map of the Lomblem sheet at a scale of 1 : 250 000, the area's lithology includes Coral Limestone, Nangapanda Formation, Viquegue Formation, Kiro Formation, and Noil Toko Formation. The Nangapanda Formation consists of rock layers such as sandy tuff, tuff breccia, and sandy limestone, formed during the Early to Middle Miocene, approximately 23–11 million years ago.

Pre-field work. The pre-field activities included data collection and the creation of a geomorphological map. The data collected comprised terrain data processed from LiDAR data with a resolution of 3 cm, land use land cover data, and rainfall data obtained from the global precipitation model (GPM) satellite for the years 2020–2023. Manual delineation of landform units was conducted at a scale of 1 : 25 000 to highlight variations in relief and morphology, referring to the classification by The National Committee on Soil and Terrain (2009). The data sources used included the national digital elevation model (resolution 8.27 m) combined with terrain data from LiDAR. Datasets for DEM were provided by Information Geospatial Information Agency (2018).

Field work. Soil sampling was conducted along transects representing landforms (geomorphic zones) and using participatory techniques to identify flood-affected areas and high flood frequency locations. Participatory techniques are more ef-

https://doi.org/10.17221/147/2024-SWR

fective in gathering disaster risk information (Pelling 2007) and enhancing resilience (Haynes et al. 2020). Sampling was performed using augers and pits at a depth of approximately 1 m in May 2023, with a total of 12 sampling points. Based on the dominant geomorphological processes in the Wei Laing watershed, geomorphic zones were identified as the erosional-transfer zone and the depositional zone (Figure 2B). The erosional-transfer zone is characterized by steep or moderately sloping terrain with arrangements of ridges, slopes, and valleys. Parent rocks in this zone consist of sandy tuffs, tuffaceous breccias, and locally intercalated sandy limestone. The soil in this zone is generally thin, with a shallow surface layer (0–30 cm). The depositional zone, typical of fluvial-marine deposition, includes residential and agricultural areas. Damage caused by debris flows and flooding resulted in significant losses during TC Seroja. The soil in this zone is moderately deep, with a surface depth ranging from 80 to over 100 cm.

Laboratory analysis. A total of 31 soil samples were tested in the laboratory to determine their physical and chemical characteristics. The soil parameters analysed included soil texture, $CaCO_3$ content, organic matter (OM), and the presence of coarse organic materials such as freshwater snail shells and coral. A geopedological approach was used to identify and compare the characteristics of each soil layer to understand their relationship with past flood events in the landforms (Zinck et al. 2016). Soil characteristics serve as a paleo-stage indicator for identifying past floods' traces. These characteristics can act as flood proxies, preserving information about historical flood events (Benito & Thorndycraft 2004; Herget 2020).

Hydrological modelling. GPM satellite rainfall data was chosen as the data source. This satellite data was chosen due to the absence of rainfall stations in the study area (Hidayah et al. 2024). The collected rainfall data was statistically analysed to determine return period values, using probability distribu-

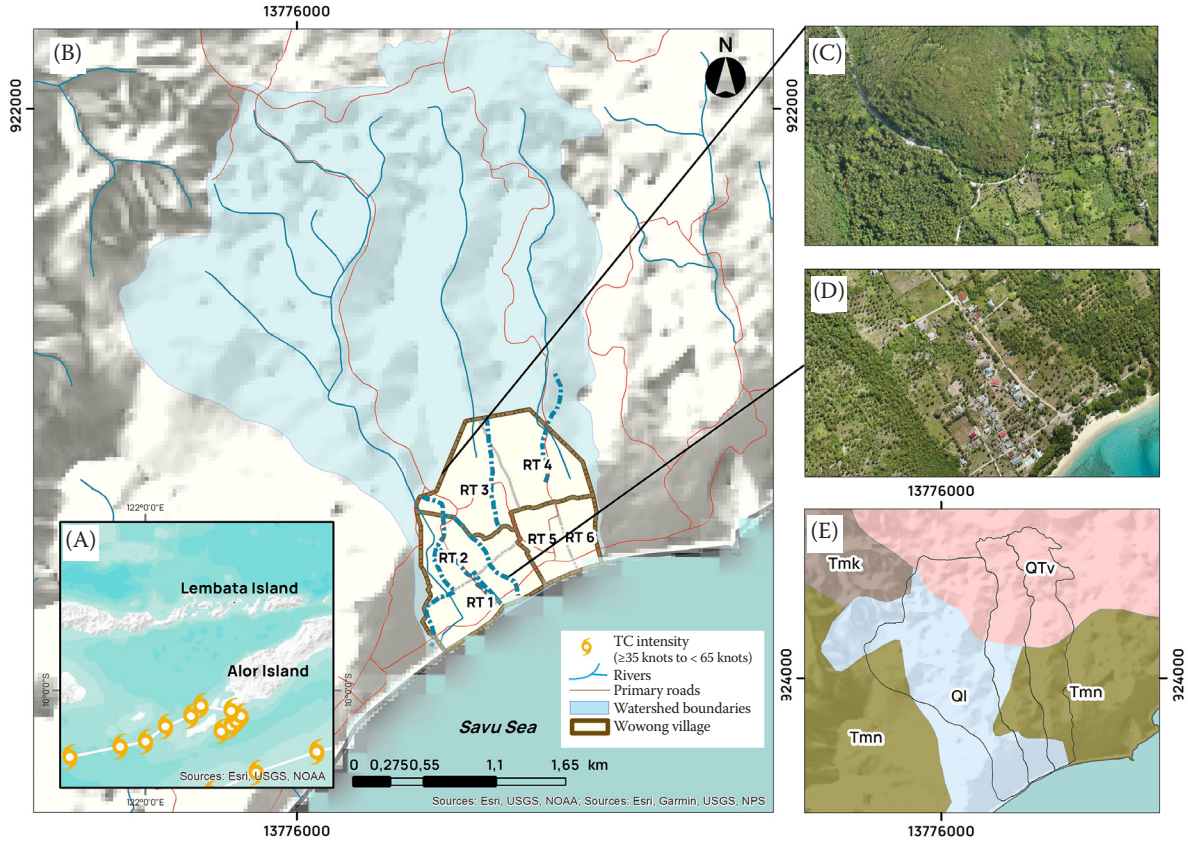

Figure 1. Tropical cyclones (TC) Seroja's track leads to Lembata and its intensity (A), Wowong Village and Wei Laing watershed (B), aerial photo of bottleneck area (2023) (C), aerial photo of the most densely populated area (2023) (D), and main lithological aspects (E)

Tmk – Tertiary Kiro Formation; Tmn – Tertiary Noil Toko Formation; Ql – Quaternary Coral Limestone; QTv – Quaternary-Tertiary Viquegue Formation

https://doi.org/10.17221/147/2024-SWR

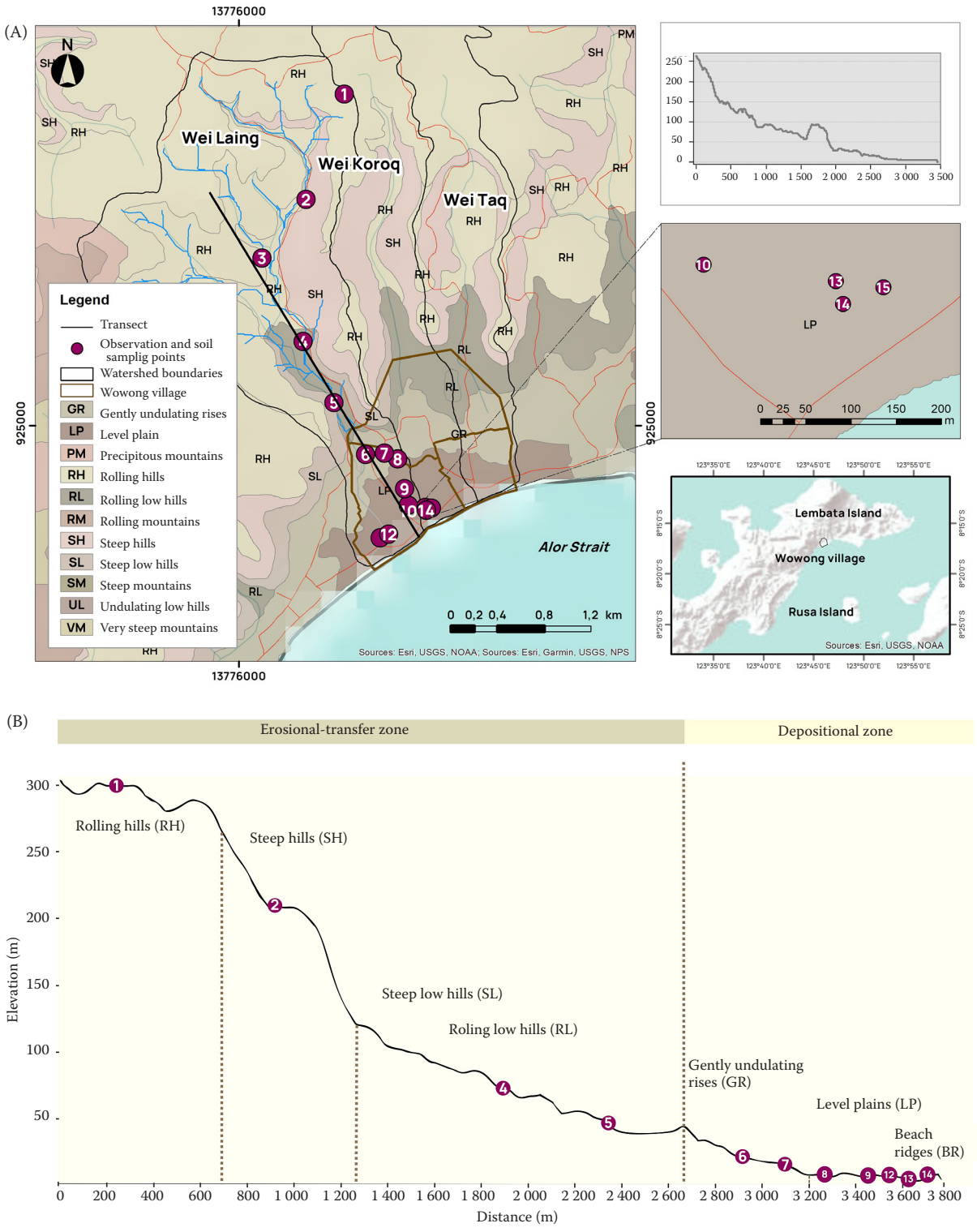

Figure 2. Soil sampling (A) and cross-sectional profile of geomorphic zones in the Wei Laing watershed (B)

tions such Log-Pearson III. These distributions were tested with Kolmogorov-Smirnov tests to identify the appropriate return period values for 2, 5, 10, 20, and 50 years, with the goal of finding values most similar to TC Seroja rainfall. The return period value represents a single event without temporal distribution, necessitating the analysis of temporal rain distribution using the Soil Conservation Service (SCS) Unit

https://doi.org/10.17221/147/2024-SWR

Hydrograph (UH) model. In this study, the SCS-(curve number) CN method is employed, accounting for land cover and soil hydrological group (Wróbel et al. 2020), producing surface runoff-a significant cause of flooding in Wowong Village. HEC-RAS software facilitates these calculations and can visualize flood inundation (Sathya & Thampi 2021).

RESULTS AND DISCUSSION

Depositional zone: TC Seroja flood deposit and paleoflood deposit. The transect perpendicular to the coastline indicates that flooding caused by TC Seroja deposited sediments up to 4 cm thick, as observed at points 13 and 14 (200 m from the coast). Flood deposits were analysed separately as a distinct type of recent flood deposit (modern deposit), whereas upstream-midstream deposits were identified as riverbank deposits and hill residuals. The morphological characteristics of the flood deposits are marked by vertical changes in colour and texture, loamy texture with very fine to coarse platy structures, and cracks on the muddy surface (Figure 3G). These thin grey flood deposits have a silty clay loam texture at point 14 and a silt loam texture at point 13, indicating fine material deposited under slow-flowing conditions. The texture transition from clay to loam is likely due to the phenomenon of reverse seasonal flooding (Wang et al. 2018). Silt deposition near the land margin occurs because of a salinity gradient trapping silt particles from freshwater in the saltwater layer as turbulence decreases. Based on their characteristics, the deposits at points 13 and 14 are identified as slackwater deposits (SWDs). Slackwater deposits are fine silt or sand deposits that rapidly accumulate from suspension during major floods in areas where local flow velocity decreases (Saynor & Erskine 1993). Organic matter content reached 11.63% at point 14

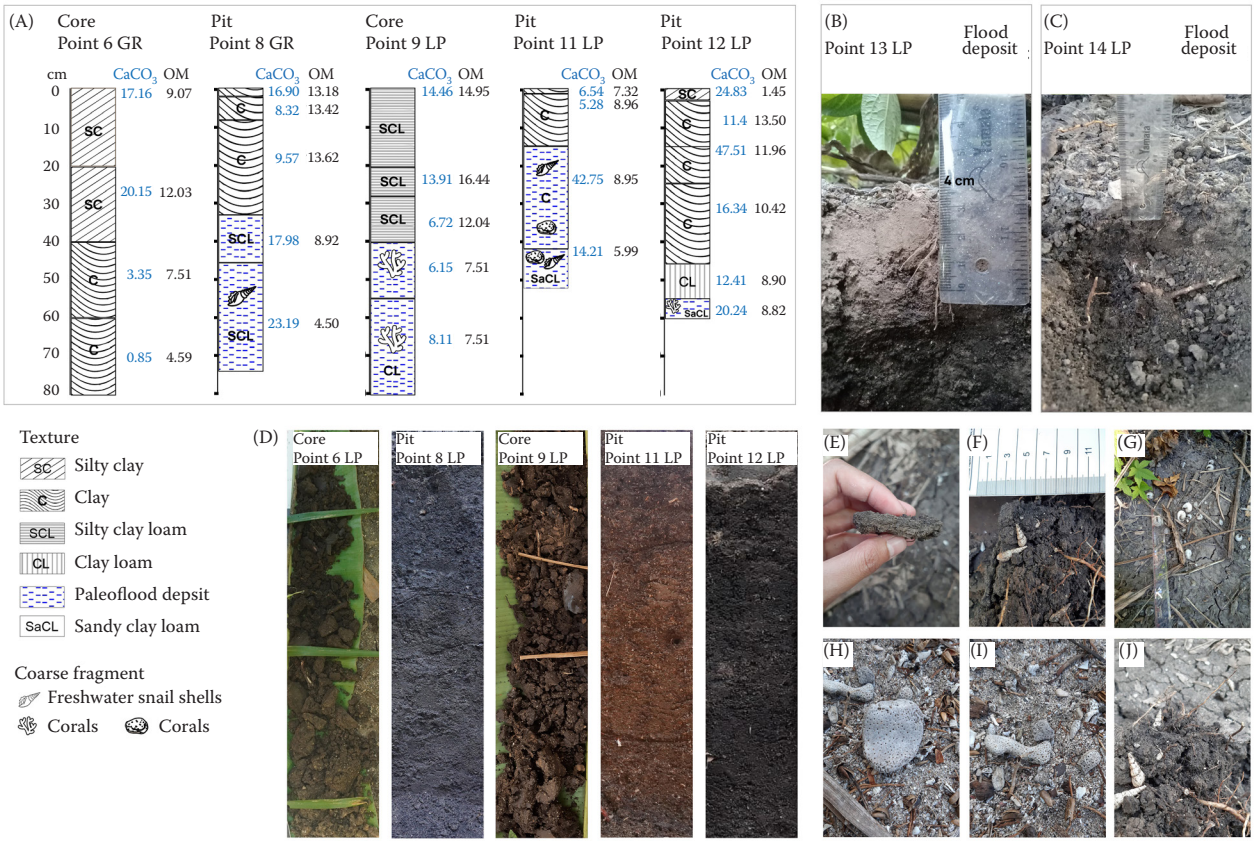

Figure 3. Soil profiles from core and pit points at several locations (GR, gently undulating rises and LP, level plain), variations in soil texture showing (A), flood deposit at point 13 LP with a thickness of approximately 4 cm (B), flood deposit at point 14 LP (C), soil profiles at various points (D), platy structure of flood deposit (E), a coarse fragment, consisting of a freshwater snail shell (F), mud cracks after flood events (G), coarse fragments of corals (H), other coarse fragments, including coral pieces (I), showing the surface is abundant with freshwater snail shells (*Allopeas gracile*) (J)

https://doi.org/10.17221/147/2024-SWR

and 14.67% at point 13, supporting the indication of material accumulation under anaerobic flood conditions (Baker 1987). The average organic matter (OM%) in soil layers within the depositional zone is approximately 9.92%, while it is 12.15% in the erosional-transfer zone. This aligns with findings by Saint-Laurent et al. (2014), which indicates that alluvial soils frequently affected by flooding tend to have lower soil organic carbon concentrations (SOC%). A significant $CaCO_3$ content (27.88%) at point 14 suggests that this mineral was deposited along with fine sediments. Other chemical properties showed no consistent patterns. As noted by Lee et al. (2014), found that soil pH may remain unchanged or increase after flooding, whereas sodium (Na) concentration and electrical conductivity tend to decrease.

Soil profile data indicate that sediment layers in this area were formed by flood deposition rather than pedogenesis. The absence of clear soil horizons emphasizes the dominance of sediment flows from flooding rather than long-term weathering processes. The layered soil texture shows significant variability in the landscape samples, with uneven distribution. The proportion of silt and clay in the 31 texture-tested samples is 80.7%. The finest deposits were found at points 6, 8, 11, and 12, with clay content exceeding 50%. Point 6 does not exhibit distinct characteristics of ancient flood deposits, but certain features, such as the presence of a silty clay layer (Figure 3A), an increase in sand, and a decrease in $CaCO_3$ content towards the lower layer, suggest the possibility of slow sedimentation processes associated with short-term water flows. At point 8 (Figure 3A), changes in texture to loam, an increase in sand content in the lower layer, and high $CaCO_3$ content in the upper and lower layers (but lower in the middle) indicate the possibility of a flood event during the deposition period (paleoflood deposit). This is further supported by the presence of freshwater snail shells (*Allopeas gracile*) at depths of 46–74 cm, confirming that the area experienced flooding (Guo et al. 2021; Lv et al. 2023).

Our data indicate a relationship between $CaCO_3$ content and OM at various sample depths, suggesting similar flood deposition processes (Table 1). Shallow layers: points 8, 9, 13, 14, and 6 likely indicate deposition from recent floods. Medium-depth layers: points 8, 12, and 6 show moderate $CaCO_3$ and OM content, possibly indicating deposition from recurring floods. Deeper layers: points 11, 12, and 6 likely represent older deposition layers. High $CaCO_3$ concentration: layers at points 11 and 5 suggest carbonate-rich sediment deposition, while the low OM content indicates deposition in high-energy environments, such as water channels at point 5 and former river flow areas at point 11.

All soil layers containing coarse organic materials are identified as paleoflood deposits with loamy textures. The presence of coral fragments in the layers at points 7 and 9 indicates the influence of coastal material transportation to deeper inland areas through flooding. The texture at point 9 shows an increase in sand content, signifying increased flow energy with depth. Coral fragments found

Table 1. Layers with similar $CaCO_3$ and organic matter (OM) levels across sample points

Layer characteristics	Point No. (depth, cm)	$CaCO_3$	OM
		(%)	
Layers with high $CaCO_3$ and OM at shallow depth (0–20 cm)	8 (0–2)	16.9	13.2
	9 (0–20)	14.5	15.0
	13 (modern deposit)	14.5	14.7
	14 (modern deposit)	27.9	11.6
	6 (0–20)	17.2	9.1
Layers with moderate $CaCO_3$ and OM at medium depth (20–40 cm)	8 (33–46)	18.0	8.9
	12 (25–46)	16.3	10.4
	6 (20–40)	20.2	12.0
Layers with low $CaCO_3$ and moderate OM at deeper depth	11 (1–15)	5.3	9.0
	12 (16–25)	7.5	12.0
	6 (40–60)	3.4	7.5
Layers with very high $CaCO_3$ and low OM	11 (15–42)	42.8	9.0
	5 (0–10)	30.9	10.3

https://doi.org/10.17221/147/2024-SWR

at point 9 (40–80 cm depth) and freshwater snail shells at point 11, located 145 meters from point 9, suggest the accumulation of coarse material inland through strong flows. Texture changes at point 12, transitioning to clay loam and sandy clay loam with sand content reaching 49.25% in the lower layer, also point to the deposition of coarse materials during high-energy flow events. The discovery of pottery shards at a depth of 55–60 cm indicates past human activity that might have been impacted by changes in flow or major flood events, further supporting the assumption of intense flow events in the past.

The coastal conditions in this area are also influenced by washover processes. Coarse materials such as coral fragments are transported over natural barriers like beach ridges and distributed into the backshore areas (Figure 3H, I). This process often occurs during major storms or high waves, where intense rainfall and increased runoff contribute to hydrodynamic changes, similar to events documented in the Gulf of Thailand (Williams et al. 2016). Changes in river flow in Wowong Village, last observed as active in 2018, have also affected the distribution of coarse sediments in this area. The river is dammed with a permanent sluice gate in the midsection of the Wei Laing watershed, near the bottleneck (point 6) (Figure 1), causing changes in the depositional environment. This area is now predominantly influenced by hydrological processes, including rainfall, surface runoff, and slow sediment deposition, which contribute to the accumulation of finer surface deposits.

Material in the upper-middle area. The upper-middle area of the Wei Laing watershed serves as an erosional transfer zone, supplying material to the deposition zone. The soil characteristic material in the upper-middle area is displayed in Figure 4. The soil characteristics at points 1–5 have shallow depths, with maximum depth of 22 cm. The shallow depth indicates that the process of pedogenesis is still limited due to the influence of geomorphological activities such as intensive erosion (Gerke et al. 2016; Wade et al. 2020). The soil texture in this area is predominantly silt with proportions ranging from 37% to 65%. This indicates that the soil particles are finer, with a relatively high water-retention capacity but inefficient drainage. Geomorphological processes such as sediment transport by river flow have increased the proportion of silt in this area, reinforcing the poor drainage characteristics (Bottcher et al. 1980), which affects the soil texture category as loam at all five points. This loam texture is similar to the floodplain soil texture at points 13 and 14. This suggests that the flood deposit source originates from the upper-middle part of the Wei Laing watershed.

The indication of flood deposit sources is further strengthened by the chemical characteristics of the soil, including $CaCO_3$ and organic matter content. Based on these characteristics, the sediment material source specifically comes from points 4 and 5, as these points have high $CaCO_3$ and organic matter content, similar to the flood deposit characteristics at points 13 and 14. Points 4 and 5 are located in rolling

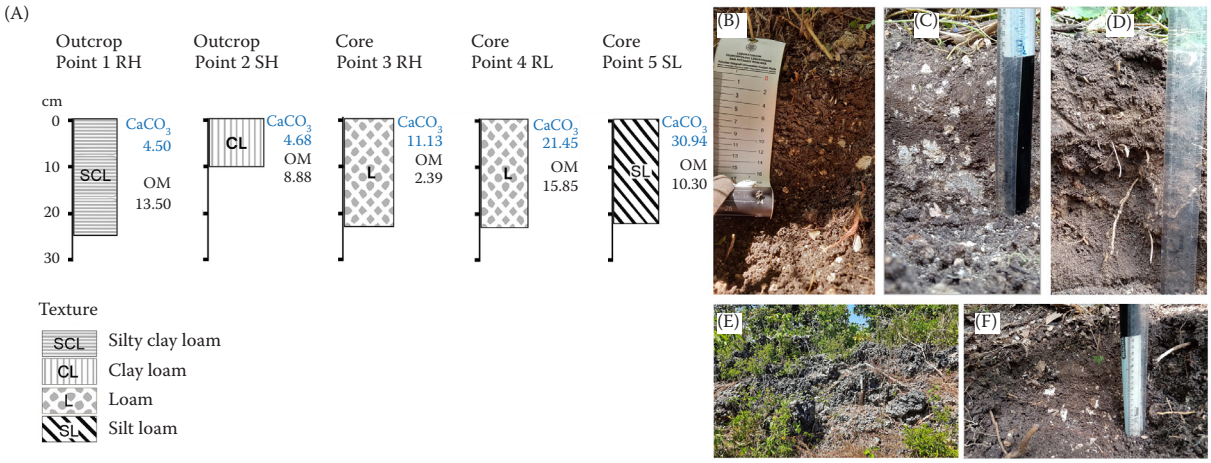

Figure 4. Soil profiles from outcrop and core points at several locations (RH, rolling hills; SH, steep hills; RL, rolling low hills; SL, steep low hills), showing variations in soil texture (A), soil thickness at point 2 (10 cm) (B), soil thickness at point 3 (22 cm) (C), soil thickness point 4 (22 cm) (D), outcrop tuf carbonate Point 1, soil thickness 22 cm (E), soil thickness at point 5 (22 cm), identified white coarse fragment between the soil (F)

https://doi.org/10.17221/147/2024-SWR

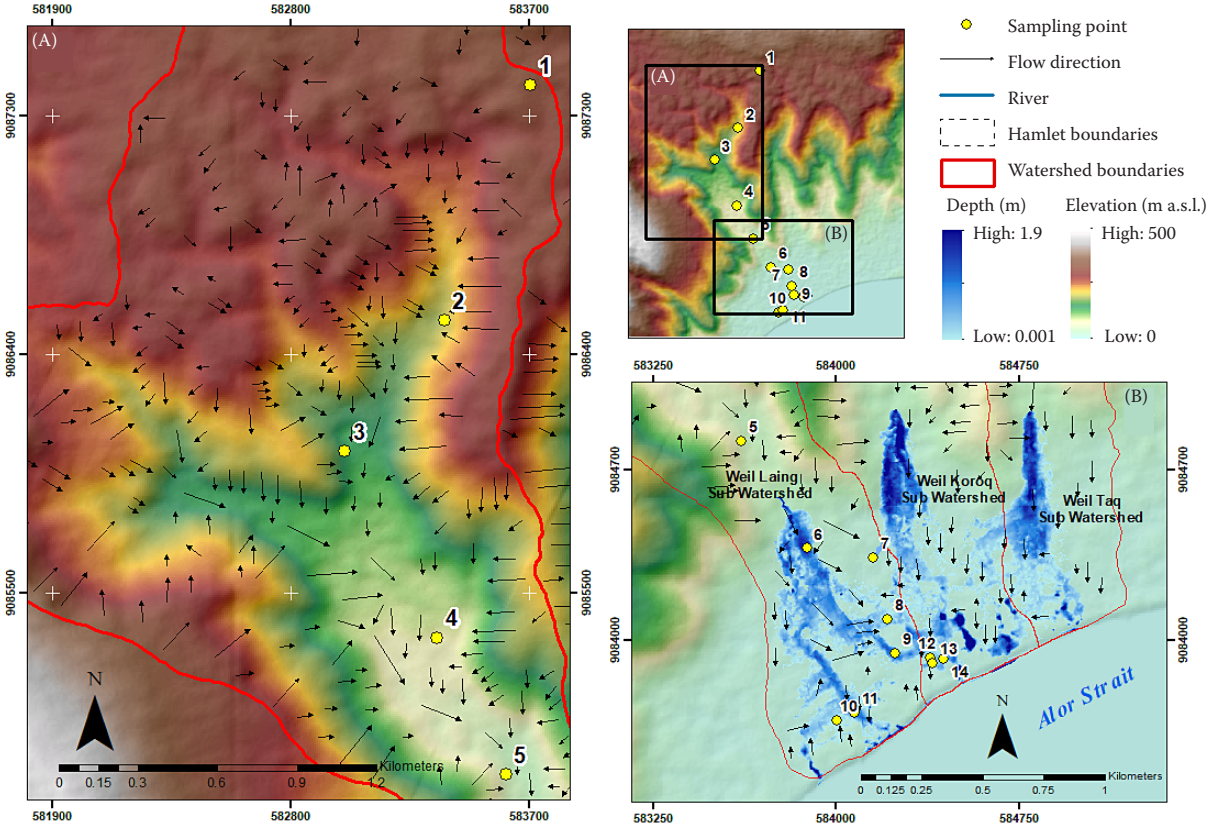

Figure 5. Map of flow direction across erosional-depositional zone (A) and inundation distribution in depositional zone that caused by 60 mm/day rainfall (B)

low hills and steep low hills with a morphoaransement of river valleys. Points 4 and 5 form a bottleneck shaped like a valley, through which the flow moves towards the lower plain. This has implications for the massive material transport process, particularly with carbonate rocks that are easily dissolved by water, influencing the soil conditions in the deposition area (Cohen et al. 2014; Wackett et al. 2018; Lin et al. 2024), in this case, in Wowong Village. The dynamics of sediment supply and transfer in the watershed are influenced by other factors such as rainfall intensity and land use, which affect erosion and sediment levels in the watershed. The high rainfall intensity caused by TC Seroja in the upper-middle part of Wei Laing watershed affected the flood deposits. The deposit has similar characteristics to the soil characteristics in the upper-middle part of the watershed. This indicates that the soil characteristics in the upper-middle part of the watershed, which has a loam texture, tends to have a high water-holding capacity, but poor drainage, thus increasing the surface runoff. The thin material in the upper region causes the flood deposits in the depositional zone to be similarly thin, as confirmed at points 13 and 14, where the deposits are only about 4 cm thick.

Hydrological modelling results. The flood deposit of 3–4 cm thick, resulting from 250 mm/day of rainfall triggered by TC Seroja, shows a recurrence probability of 2%. This probability was derived from a frequency analysis of daily rainfall from 2000 to 2023. The frequency analysis using the Log-Pearson III method indicated a value of 247 mm/day for a 50-year return period, with 5% level of significance.

The flow direction model results (Figure 5A) show that the runoff from the rainfall accumulates in local valleys. In the 50-year return period review, the maximum discharge in the Wei Laing sub watershed, Wei Koroq sub watershed, and Wei Taq sub watershed were 38.40, 16.83, and 20.02 m^3/s, respectively, entering the Wowong Village. The Wei Laing sub-watershed has the largest area compared to the other two sub watersheds, resulting in the highest discharge. With nearly identical land cover and slope conditions, the morphometry of the sub-watershed

https://doi.org/10.17221/147/2024-SWR

Table 2. Curve number (CN) composition in Wei Laing Sub-watershed

HSG	LC	Area (km^2)	CN value	Composite CN
B	woody savanna	2.74	71	80
	savanna	0.05	80	
D	woody savanna	1.91	89	
	savanna	0.40	93	

HSG – hydrologic soil group; LC – land cover

plays a role in quantifying discharge at the sub watershed outlet (Romshoo et al. 2012). A more detailed review reveals that the upstream area of the Wei Laing sub-watershed consists of land cover (LC) types primarily categorized as woody savanna and savanna. Additionally, this region falls within hydrologic soil group (HSG) B and D. As a result, the area exhibits curve number (CN) values, as presented in Table 2. Based on CN values, surface runoff is most prevalent in HSG D with the savanna LC class. The composite CN value of 80 suggests a significant potential for surface runoff. With a CN of 80, the expected runoff volume from a rainfall event is relatively high. The increased runoff volumes associated with this CN value can contribute to heightened soil erosion and sediment transport, as greater water movement over the land surface enhances the detachment and mobilization of soil particles.

Other flood deposits (not from TC Seroja) are indicated to have formed due to rainfall with lower intensity than that of TC Seroja. Running simulations in HEC-RAS with different rainfall intensities showed that all sampling points started to flood when the rainfall intensity reached 60 mm/day (Figure 5B). Based on the model, 60 mm/day rainfall is identified as the minimum threshold for flood events in Wowong Village.

Further analysis of the relationship between daily rainfall data from 2000 to 2023 and the minimum flood threshold indicates that there have been 77 flood events. The majority of these floods were caused by rainfall with a return period of less than 2 years, occurring within the rainfall intensity range of 60 to 97.6 mm/day. A total of 60 events, or 77.9% of all events, occurred within this return period. Furthermore, of the 77 recorded flood events, 76 were not caused by TC Seroja, accounting for 98.7% of all occurrences (Figure 6). These percentages are believed to contribute to the formation of deposits at the soil sampling points.

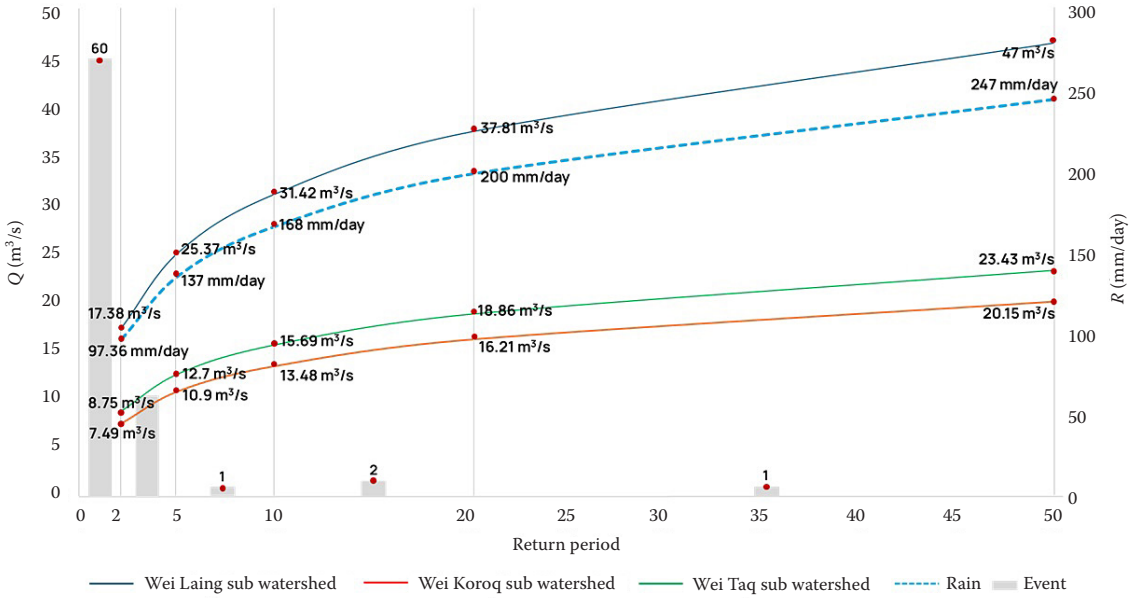

Figure 6. Relationship between rainfall discharge and the number of rain events in Wowong Village
Q – discharge; *R* – rainfall

https://doi.org/10.17221/147/2024-SWR

The majority of rainfall events ≥ 60 mm/day occur during the wet months, specifically from November to April. The increase in rainfall intensity during this period is strongly related to the phenomenon of the west monsoon winds (Alsepan & Minobe 2020). In contrast, from May to October, rainfall is rare, with the most significant cause being the activity of the east monsoon winds. However, despite the important role of the monsoon winds in the distribution of rainfall, it is also possible that rainfall events ≥ 60 mm/day could be caused by tropical cyclones. This is due to the geographical location of the Wei Laing watershed, which is situated at 8°S.

CONCLUSION

The key to interpreting the physical and chemical characteristics of soil to recognize flood deposits includes the analysis of texture, $CaCO_3$ content, organic matter, and coarse organic material deposits. Modern flood deposits (TC Seroja deposits) can be identified as slackwater deposits with a thickness of ≤ 4 cm, while paleoflood deposits can also be identified by thicker deposits of coarse organic material. However, these interpretive keys are not sufficient for comprehensively identifying flood evidence. This indicates the need for additional data integration, such as grain size analysis, geochemistry, and carbon dating. To support the finding that the area is composed of flood deposits, hydrological modelling is required. Through recurrence period calculations, rainfall with an intensity similar to TC Seroja (250 mm/day) is identified as a 50-year return period rainfall. This suggests that the event is extreme and rare. The HEC-RAS model shows that the minimum rainfall threshold causing flooding in Wowong Village is 60 mm/day, with all sampling points being inundated. Based on this threshold, between 2000 and 2023, Wowong Village experienced 77 flood events. This supports the conclusion that the soil formed in the Wowong Village is the result of flood deposition.

Acknowledgements. The authors would like to thank Universitas Gadjah Mada for supporting this research and its funding. We express our sincere gratitude to the Center for Disaster Studies UGM and Yayasan PLAN International Indonesia for their valuable guidance. Special thanks go to Yuli Widyaningsih, Ariel Seto Adinugraha, and Mila Siti Fatimah for their significant contributions and support throughout this project.

REFERENCES

Alsepan G., Minobe S. (2020): Relations between interannual variability of regional-scale Indonesian precipitation and large-scale climate modes during 1960–2007. Journal of Climate, 33: 5271–5291.

Baker V.R. (1987): Paleoflood hydrology and extraordinary flood events. Journal of Hydrology, 96: 79–99.

Ballesteros-Canovas J.A., Bombino G., D'Agostino D., Denisi P., Labate A., Stoffel M., Zema D.A., Zimbone S.M. (2020): Tree-ring based, regional-scale reconstruction of flash floods in Mediterranean mountain torrents. Catena, 189: 104481.

Benito G., Thorndycraft V.R. (2004): Systematic, Palaeoflood and Historical Data for the Improvement of Flood Risk Estimation: Methodological Guidelines. Madrid, CSIC – Centro de Ciencias Medioambientales.

Bottcher A.B., Monke E.J., Huggins L.F. (1980): Subsurface drainage and sediment transport model. Transactions, American Society of Agricultural Engineers, 23: 870–876.

Bureau of Meteorology (2023): Tropical Cyclones – Past Cyclones. Available on https://www.bom.gov.au/cyclone/history/

Chen G., Li G., Liu M., Luo K., Huang Y., Bao C., Zhan C. (2024): Paleo-tropical cyclone activity over the last millennium inferred from shipwreck relics in the Xisha Islands, northern South China Sea. Marine Geology, 471: 107288.

Cohen S., Willgoose G., Svoray T., Hancock G., Sela S. (2014): The effects of sediment transport, weathering, and aeolian mechanisms on soil evolution. Journal of Geophysical Research: Earth Surface, 120: 260–274.

Denniston R.F., Luetscher M. (2017): Speleothems as high-resolution paleoflood archives. Quaternary Science Reviews, 170: 1–13.

Dong W.S., Ismailluddin A., Yun L.S., Ariffin E.H., Saengsupavanich C., Abdul Maulud K.N., Ramli M.Z., Miskon M.F., Jeofry M.H., Mohamed J., Mohd F.A., Hamzah S.B., Yunus K. (2024): The impact of climate change on coastal erosion in Southeast Asia and the compelling need to establish robust adaptation strategies. Heliyon, 10: e25609.

Donnelly J.P., Hawkes A.D., Lane P., MacDonald D., Shuman B.N., Toomey M.R., van Hengstum P.J., Woodruff J.D. (2015): Climate forcing of unprecedented intense-hurricane activity in the last 2000 years. Earth's Future, 3: 49–65.

Eberenz S., Lüthi S., Bresch D.N. (2021): Regional tropical cyclone impact functions for globally consistent risk assessments. Natural Hazards and Earth System Sciences, 21: 393–415.

https://doi.org/10.17221/147/2024-SWR

Fahrudin A., Patrianti T., Yusuf H. (2022): Climate change, disaster, and social work in Indonesia. In: Baikady R., Przeperski J., Islam M.R., Sakaguchi S.M. (eds.): The Palgrave Handbook of Global Social Problems. Cham, Palgrave MacMillan: 1–14.

Geospatial Information Agency (2018): Tanah Air Indonesia. Available on https://tanahair.indonesia.go.id/

Gerke H.H., Rieckh H., Sommer M. (2016): Interactions between crop, water, and dissolved organic and inorganic carbon in a hummocky landscape with erosion-affected pedogenesis. Soil and Tillage Research, 156: 230–244.

Guo S.Y., Li L., Zhang L.J., Li Y.L., Li S.Z., Xu J. (2021): From the one health perspective: Schistosomiasis Japonica and flooding. Pathogens, 10: 1–12.

Haynes K., Bird D.K., Whittaker J. (2020): Working outside 'the rules': Opportunities and challenges of community participation in risk reduction. International Journal of Disaster Risk Reduction, 44: 101396.

Herget J. (2020): Palaeostage Indicators in Rivers – An Illustrated Review. Palaeohydrology. Geography of the Physical Environment. Cham, Springer.

Hidayah E., Saifurridzal S., Wiyono R.U.A., Widiarti W.Y., Martini R., Juliastuti J., Riduwan M. (2024): Performance of GPM-IMERG satellite precipitation for rainfall-runoff modeling in Indonesia. Water Practice & Technology, 19: 3909–3928.

Janakiraman A., Sudhakar M.P., Ratnam K., Santhanakumar J., Jha D.K., Dharani G. (2024): An impact of tropical cyclone on meiobenthic fauna of Chennai coast, Tamil Nadu, India: A case study of cyclone Mandous. Science of the Total Environment, 918: 170657.

Kurniawan R., Harsa H., Nurrahmat M.H., Sasmito A., Florida N., Makmur E.E.S., Swarinoto Y.S., Habibie M.N., Hutapea T.F., Hendri Sudewi R.S., Fitria W., Praja A.S., Adrianita F. (2021): The impact of Tropical Cyclone Seroja to the rainfall and sea wave height in East Nusa Tenggara. IOP Conference Series: Earth and Environmental Science, 925: 0–12.

Latos B., Peyrillé P., Lefort T., Baranowski D.B., Flatau M.K., Flatau P.J., Riama N.F., Permana D.S., Rydbeck A.V., Matthews A.J. (2023): The role of tropical waves in the genesis of Tropical Cyclone Seroja in the Maritime Continent. Nature Communications, 14: 1–12.

Lee H., Alday J.G., Cho K.H., Lee E.J., Marrs R.H. (2014): Effects of flooding on the seed bank and soil properties in a conservation area on the Han River, South Korea. Ecological Engineering, 70: 102–113.

Lin Z., Huang W., Liao D., Deng Y. (2024): Sediment production process and hydraulic characteristics of ephemeral gully erosion in granite hilly area. Catena, 239: 107946.

Lv S.B., He T.T., Hu F., Li Y.F., Yuan M., Xie J.Z., Li Z.G., Li S.Z., Lin D.D. (2023): The impact of flooding on snail spread: The case of endemic schistosomiasis areas in Jiangxi Province, China. Tropical Medicine and Infectious Disease, 8: 259.

Minamidate K., Goto K. (2024): Unveiling the history and nature of paleostorms in the Holocene. Earth-Science Reviews, 253: 104774.

Mulyana E., Prayoga M.B.R., Yananto A., Wirahma S., Aldrian E., Harsoyo B., Seto T.H., Sunarya Y. (2018): Tropical cyclones characteristic in southern Indonesia and the impact on extreme rainfall event. MATEC Web of Conferences, 229: 02007.

National Committee on Soil and Terrain (2009): Australian Soil and Land Survey Field Handbook. 3rd Ed. Collingwood, CSIRO Publishing.

Nott J. (2004): Palaeotempestology: The study of prehistoric tropical cyclones – A review and implications for hazard assessment. Environment International, 30: 433–447.

Pelling M. (2007): Learning from others: The scope and challenges for participatory disaster risk assessment. Disasters, 31: 373–385.

Rodysill J.R., Donnelly J.P., Sullivan R., Lane P.D., Toomey M., Woodruff J.D., Hawkes A.D., MacDonald D., d'Entremont N., McKeon K., Wallace E., van Hengstum P.J. (2020): Historically unprecedented Northern Gulf of Mexico hurricane activity from 650 to 1250 CE. Scientific Reports, 10: 1–17.

Romshoo S.A., Bhat S.A., Rashid I. (2012): Geoinformatics for assessing the morphometric control on hydrological response at watershed scale in the Upper Indus Basin. Journal of Earth System Science, 121: 659–686.

Saint-Laurent D., Gervais-Beaulac V., Berthelot J.S. (2014): Variability of soil properties in different flood-risk zones and link with hydroclimatic changes (Southern Québec, Canada). Geoderma, 214–215: 80–90.

Sathya A., Thampi S.G. (2021): Flood inundation mapping of Cauvery River using HEC-RAS and GIS. In: Singh R.M., Sudheer K.P., Kurian B. (eds): Advances in Civil Engineering. Lecture Notes in Civil Engineering, Vol 83. Singapore, Springer.

Saynor M.J., Erskine W.D. (1993): Characteristics and implications of high-level slackwater deposits in the Fairlight Gorge, Nepean river, Australia. Marine and Freshwater Research, 44: 735–747.

Sekaranom A.B., Putri N.H., Puspaningrani F.C. (2021): The impacts of Seroja Tropical Cyclone towards extreme weather in East Nusa Tenggara. E3S Web of Conferences, 325: 01020.

Shashank V.G., Sriram V., Schüttrumpf H., Sannasiraj S.A. (2024): A new surge index with the incorporation of cyclone track approach angle information for the Bay of Bengal. Coastal Engineering, 188: 104429.

https://doi.org/10.17221/147/2024-SWR

Stanton-Geddes Z., Vun Y.J. (2019): Strengthening the Disaster Resilience of Indonesian Cities. In: Roberts M., Gil Sander F., Tiwari S. (eds.): Time to ACT: Realizing Indonesia's Urban Potential. Washington, D.C., World Bank: 161–171.

Wackett A.A., Yoo K., Amundson R., Heimsath A.M., Jelinski N.A. (2018): Climate controls on coupled processes of chemical weathering, bioturbation, and sediment transport across hillslopes. Earth Surface Processes and Landforms, 43: 1575–1590.

Wade A.M., Richter D.D., Cherkinsky A., Craft C.B., Heine P.R. (2020): Limited carbon contents of centuries old soils forming in legacy sediment. Geomorphology, 354: 107018.

Wang Y., Chen F., Zhang M., Chen S., Tan X., Liu M., Hu Z. (2018): The effects of the reverse seasonal flooding on soil texture within the hydro-fluctuation belt in the Three Gorges reservoir, China. Journal of Soils and Sediments, 18: 109–115.

Williams H., Choowong M., Phantuwongraj S., Surakietchai P., Thongkhao T., Kongsen S., Simon E. (2016): Geologic records of Holocene typhoon strikes on the Gulf of Thailand coast. Marine Geology, 372: 66–78.

Wróbel M., Mańk K., Krysztofiak-Kaniewska A. (2020): Applying the stocking index to the determination of the curve number parameter in the forest catchment area. Natural Resource Modeling, 33: e12241.

Zinck J.A., Metternicht G., Bocco G., Del Valle H. (2016): Geopedology. An Integration of Geomorphology and Pedology for Soils and Landscape Studies. Washington, D.C., Springer.

Received: December 2, 2024
Accepted: February 24, 2025
Published online: March 31, 2025